

Filtering DRA Array and Its Applications in MIMO for Sub-6 GHz Band

Suparna BALLAV, Goffar Ali SARKAR, Susanta Kumar PARUI

Dept. of Electronics & Tele-comm. Engineering, Indian Institute of Science Engineering and Technology, Shibpur, Howrah-711103, India

ballav.suparna@gmail.com, arkapv@yahoo.com

Submitted September 3, 2020 / Accepted February 12, 2021

Abstract. *A dielectric resonator-based filtering array antenna along with multi input-multi output (MIMO) characteristics is represented in this paper. Two rectangular dielectric resonators, together with a filtering power splitter (PS) is used to get a high gain filtering response. The PS, which consists of a simple T-junction 3-dB power splitters and two pairs of band-rejection resonators, provides four transmission zeros outside the passband. Detail study with an equivalent circuit is presented to understand the working principle of the filtering PS. By utilizing this PS, a two element DRA array is designed at sub-6 GHz frequency band (3.20 GHz–3.54 GHz) with an average broadside gain of 7.8 dBi in the passband and four radiation dips outside the passband. The proposed filtering DRA array effectively suppresses the out-of-band signal, delivers sharp selectivity at band edges. Finally, coalescing the two-filtering array, a MIMO antenna system is presented here. The filtering array MIMO antenna gives reasonable port isolation of greater than 20 dB throughout the operating band. All the major diversity parameters to establish MIMO characteristics e.g. envelope correlation coefficient (ECC), diversity gain (DG), channel loss capacity (CCL), and total reflection coefficient (TARC) persist within their tolerable ranges.*

Keywords

Array, filtering power splitter, high gain, radiation dip, filtering MIMO

1. Introduction

One of the acute concerns in communication systems is the overlapping caused by the harmonics. For the last few years, filters and antenna are co-designed in a single system to overcome the insertion losses and make a compact structure. Overlapping between adjacent operating frequency bands can also be effectively removed by the co-design approach [1–3]. Filtering antenna response is established using the co-design technique without any use of matching circuitry which leads to a more straightforward

design [4–6]. An open-loop resonator bandpass filter (BPF) is integrated for the filtering response of a printed monopole antenna in [4]. In [5], an arc-slot antenna is cascaded with an ultra-wideband (UWB) filter to enhance the selectivity away from passband. In [6], integration of a Vivaldi antenna with a capacitively loaded loop (CLL) resonator BPF produces a filtenna. Furthermore, the antenna array has become widely used for high gain antenna applications. High gain antenna arrays are mainly required to compensate the large free-space path losses and for well directive communication. As power divider is required for designing antenna array complexity arises in the feed network, resulting in unexpected resonances. One can resolve this issue by developing a band selective feed network for antenna array [7–9]. In [7], filtering antenna elements and filtering feed networks are combined to realize a filtering patch antenna array. Eight-element filtering planar antenna array with reduced sidelobe level is presented in [8]. A resonator-based four-port power divider is coupled with the 2×2 patch antenna array for accomplishing a fourth-order filtering response [9].

In the meantime, dielectric resonator antennas (DRAs) become popular in the late '90s for their various advantages like the absence of conduction loss, high radiation efficiency, etc. DRAs consist of a low loss ceramic volumetric assembly of multiple geometries such as rectangular, cylindrical, triangular, spherical, etc. and excite via numerous feeding techniques [10], [11]. In recent times some research groups are working on filtering DRAs [12–18]. A filtering DRA with high gain is achieved using parasitic strips in [12]. A stacked DRA with higher order mode is used to accomplish a broadband filtering antenna in [13]. The hybrid feeding technique is applied to obtain filtering DRAs in [14–16]. A quasi-isotropic filtering DRA and a circular polarized filtering DRA have been proposed very recently in [17], [18] with two radiation nulls in the gain response. Silver coated slots are incorporated to obtain a narrow band filtering DRA in [19]. A third order filtering feed network is integrated with a rectangular DRA to achieve filtering gain response in [20]. Again, with the speedy revolution of wireless systems, researchers are recommended multi input-multi output antennas. MIMO antennas are able to produce high data rate and high chan-

nel capacity, even in the existence of multipath fading. Low-loss and high gain DRA arrays could be a better choice to design MIMO antenna system, which can compensate free-space path losses [21–24].

In this paper, a two element DRA array with filtering gain characteristics is developed for sub-6 GHz applications, and this design is further extended to design a two port multi input-multi output (MIMO) antenna. A simple T-junction 3-dB power splitter integrated with two pairs of band-rejection resonators is used as a feedline for the array. Two DRA elements are placed over the ground plane at a separation of $0.53\lambda_0$ and energized through rectangular slots in the ground plane. The array operates over the frequency band of 3.2 GHz–3.54 GHz with a high broadside gain of 7.8 dBi. The proposed array shows sharp band-edges selectivity with two radiation dips on either side of passband, and the out-of-band suppression level is less than -25 dB. Finally, two filtering DRA arrays are positioned opposite to each other to develop a two-port filtering MIMO DRA array. The response of the MIMO DRA array is studied thoroughly in terms of port isolation (> 20 dB), $ECC < 0.008$, $DG > 9.99$, $CCL < 0.3$ and $TARC < -15$ dB to validate its reliability. The MIMO DRA array poses high gain with adequate in-band MIMO performance. Simulation results are verified through the fabrication and measurement of the filtering MIMO DRA array.

2. Design Methodology of Filtering DRA Array

The design principle of filtering DRA array is described in this section. First, the formation of 3-dB filtering PS is shown and then the configuration of the two elements filtering DRA array is described in detail.

2.1 3-dB Filtering Power Splitter

The conventional T-junction PS with a quarter-wave transformer is considered in this paper for division and supply of equal power to the radiating elements. The conventional T-junction PS is designed at a center frequency of 3.4 GHz. The band-edge selectivity of the power-splitter is improved by coalescing two pairs of band rejection resonators in the 1st stage of the PS and marked as input filtering stage (IFS) in Fig. 1(a). The S-parameters in Fig. 1(b) depict a filtering performance with four transmission zeros (TZs) at 2.5 GHz, 2.82 GHz, 3.8 GHz and 4.3 GHz outside the operating band. A sharp band-edge response is observed compared with the conventional PS (Conv.PS).

One can control the TZs as per requirement by changing the dimension of the resonators. The input filtering stage (IFS) of the PS containing the resonators is represented using an equivalent circuit model and the response of the circuit is compared with the response of electromagnetic simulator as given in Fig. 2(a-b). Values of L_i , C_i , L_u , C_u are determined from (1) and (2) as given in [25], [26]:

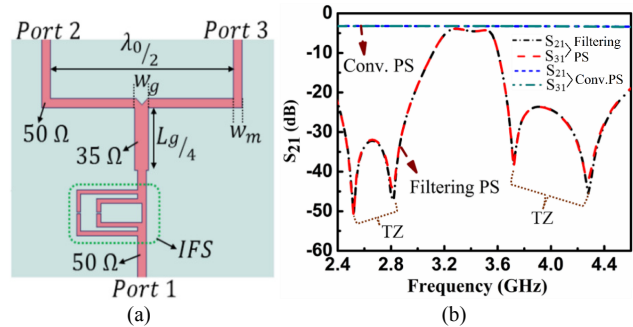


Fig. 1. (a) Layout of the 3-dB filtering power splitter (Parameters: $L_g/4 = 14.4$, $w_g = 3.45$, $w_m = 2.1$. Unit: mm). (b) Simulated S-parameter responses.

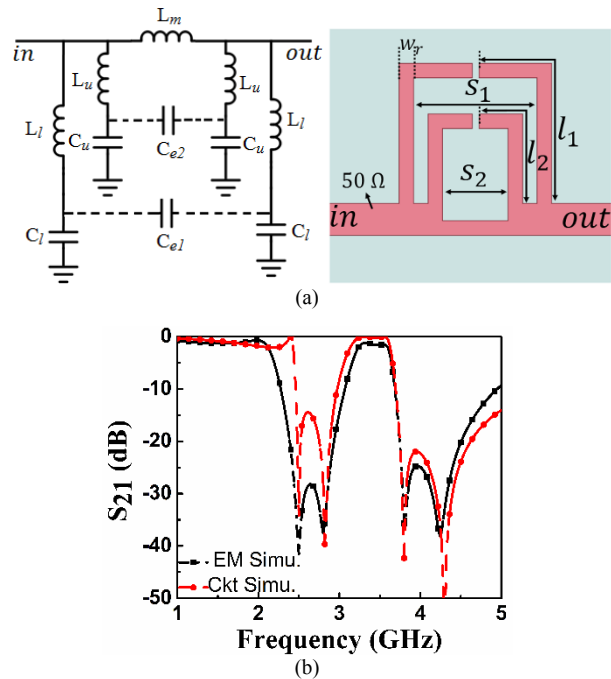


Fig. 2. (a) Layout of Input Filtering Stage (IFS) (Parameters: $S_1 = 8.5$, $S_2 = 4.5$, $l_1 = 20.6$, $l_2 = 13.1$, $w_r = 1$. Unit: mm) (b) Equivalent circuit representation along with frequency response.

$$\omega_{z1} = \frac{1}{\sqrt{L_i C_1}}, \quad \omega_{z2} = \frac{1}{\sqrt{L_u C_u}} \quad (1), (2)$$

where ω_{z1} and ω_{z2} are the resonance frequencies of lower and upper TZ, respectively. The coupling capacitors (C_{e1} and C_{e2}) and the inductor (L_m) are judiciously tuned to allocate the TZs at preferred position. The evaluated values of L and C are: $L_i = 6.2$ nH, $C_1 = 0.55$ pF, $L_u = 2.75$ nH, $C_u = 0.55$ pF, $L_m = 1.5$ nH, $C_{e1} = 0.03$ pF, $C_{e2} = 0.015$ pF, respectively.

2.2 2-Element Filtering DRA Array

Two elements filtering DRA array configuration is illustrated in Fig. 3(a). Two rectangular DRAs (RDRAs) are placed over the ground plane at a spacing of $0.53\lambda_0$ (center-to-center), where λ_0 is the wavelength corresponding to the center frequency of 3.37 GHz. The individual RDRAs have

a length/width (w_{dr}) and height (h_{dr}) of 18.5 mm, 15.3 mm respectively and dielectric material has the dielectric constant 10 and loss tangent 0.002. These RDRA sizes are primarily evaluated using the formulas in [14] for the generation of TE_{111} mode at 3.37 GHz. The DRAs are energized by two coupling slots engraved on the ground plane and the filtering fed line is printed at the bottom surface of the substrate. A low loss both-sided copper cladded Arlon material with dielectric permittivity 2.7, thickness 0.79 mm, length $l_{sb} = 110$ mm and width $w_{sb} = 80$ mm is used as substrate. All the dimensions of the array configuration are stated in Fig. 3(a). Variation of mutual coupling (S_{21}) between inter-element of the array with distance is plotted in Fig. 3(b). The center-to-center distance between the two elements is varied from $0.3\lambda_0$ to $0.8\lambda_0$. It is apparent that

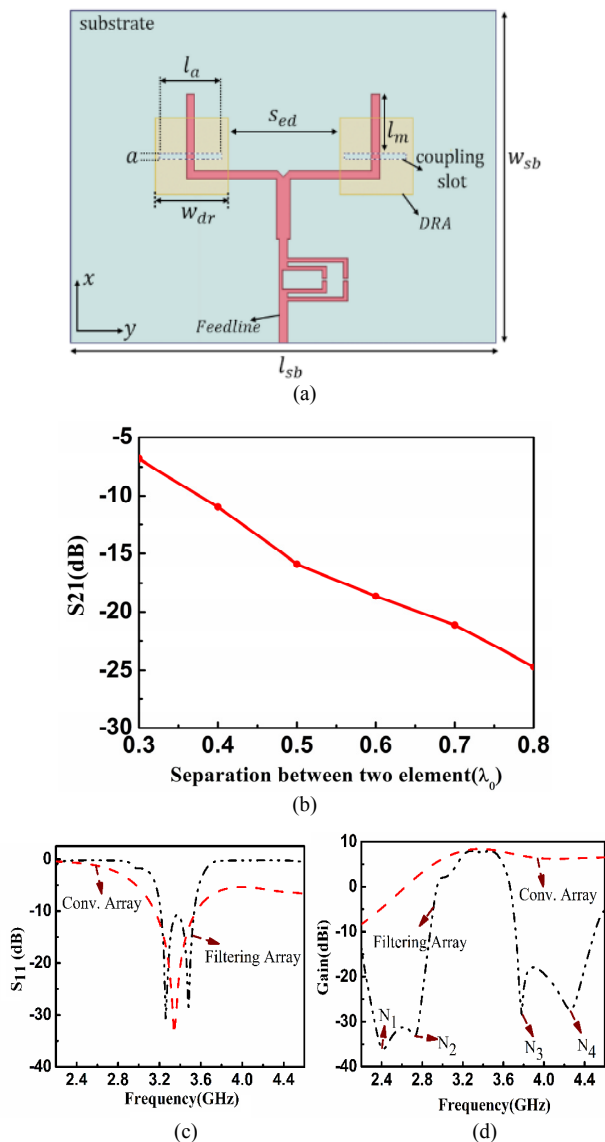


Fig. 3. (a) Layout of the 2-element filtering DRA array. (Parameters: $l_a = 16$, $l_m = 14.25$, $a = 1.5$, $S_{ed} = 29.3$. Unit: mm). (b) Simulated mutual coupling versus center-to-center distance between two elements; Comparison of (c) simulated S_{11} and (d) gain response of the conventional DRA array and the proposed filtering DRA array.

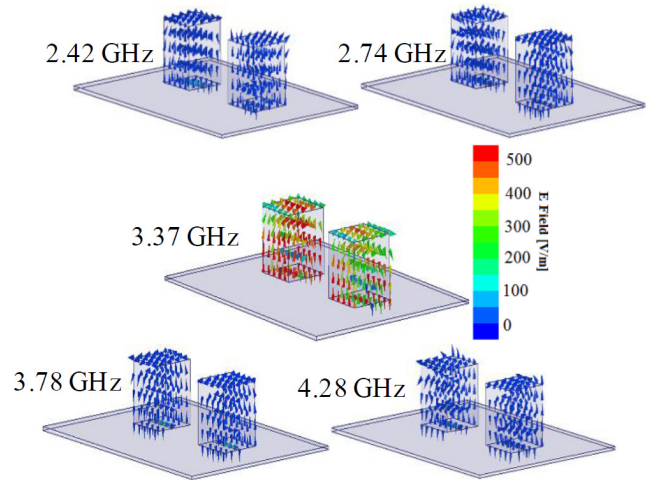


Fig. 4. E-field variation within the radiators of the filtering array at four radiation dips and center frequency Filtering MIMO DRA.

$0.5\lambda_0$ separation between the two elements at 3.37 GHz, a 15-dB coupling level is achieved. Spacing between the array elements is kept at $0.53\lambda_0$, which gives a stable broadside gain pattern. Simulated S_{11} and gain response are plotted in Fig. 3(c-d) to differentiate the conventional 2-element DRA array (conv. array) with the proposed filtering DRA array. All the parameters of the conv. array are identical except that the IFS is excluded from the feedline.

It can be observed that both the antenna operates at the center frequency of 3.37 GHz. Dissimilar loading in the feed splits the resonant frequency of TE_{111} mode of RDRA in the proposed design; hence multiple resonances are obtained in closed proximity. S_{11} response reaches sharply to 0 dB beyond the operating band and this ensures decent filtering behavior of the proposed array. The frequency selective nature of this array can also be confirmed from the frequency vs gain plot. Acute transition in the gain plot at the band-edge with four radiation dips (N_1, N_2, N_3, N_4) at 2.42 GHz, 2.74 GHz, 3.78 GHz, 4.28 GHz respectively are evident in Fig. 3(d). No such band-edge transition is noticed in conv. array. The out-of-band gain is suppressed to less than -31 dB in the lower stopband and -17 dB in the upper stopband. E-field distributions within the DRA are plotted in Fig. 4. Fields intensity inside the DRA at frequencies of four radiation dips is nearly zero; hence the radiation at those frequencies is insignificant. Whereas the E-field distribution inside the DRA at the center frequency 3.37 GHz demonstrates the proper excitation of TE_{111} mode of RDRA.

2.3 Filtering MIMO DRA Array

A two-port filtering MIMO DRA array is designed by placing the array antenna discussed in Sec. 2.2. In literature [27], [28], interlaced topology is used to design MIMO antenna system. From [28], one can find that for interlaced MIMO array antenna reasonable port isolation can be achieved either by increasing the spacing between the array

element or introducing some isolation circuits. An increase in inter-element spacing may cause higher sidelobe level, tilted main beam. As our aim is to obtain a stable broadside gain with sharp filtering response, a face-to-face placement

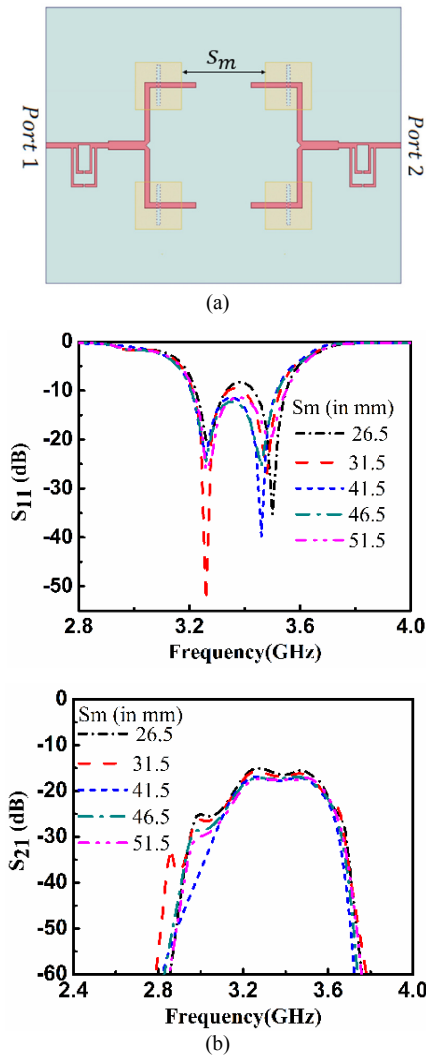


Fig. 5. (a) Layout of the proposed two port filtering MIMO DRA array. (b) S-parameters plot with the variation of S_m .

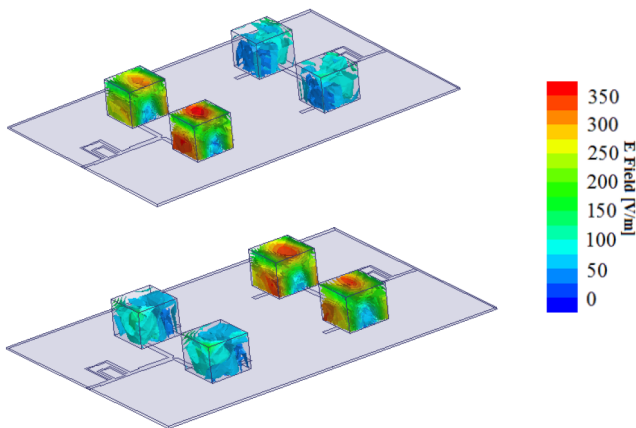


Fig. 6. E-fields variation within DRAs at 3.37 GHz. Port-1 is excited and Port-2 is terminated with matched load and vice-versa.

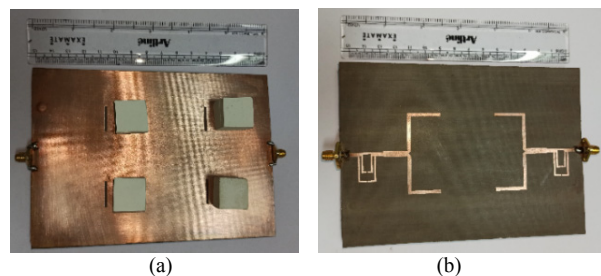
of the array is considered in this paper. Two filtering DRA arrays are placed opposite to each other at a separation of S_m . This technique provides a reasonable amount of port isolation and stable gain pattern without increasing the inter-element spacing and any use of extra isolation circuits. The proposed MIMO antenna structure is displayed in Fig. 5(a) and S-parameters for different values of S_m are shown in Fig. 5(b). It is noticeable that $|S_{11}|$ is as similar as the single port filtering array antenna and the values of port isolation parameters ($|S_{12}|/|S_{21}|$) are less than -17 dB throughout the operating band for $S_m = 46.5$ mm. E-field distributions within the radiating elements of this MIMO antenna at 3.37 GHz are shown in Fig. 6. Here, Port 1 is energized and Port 2 is terminated with 50Ω impedance and vice versa. It can be easily visualized that a sufficient amount of energy is coupled to the radiators associated with Port 1, whereas the field intensity of the radiators related to Port 2 is extremely low. As a result, port isolation values remain within a tolerable range.

3. Fabrication and Measurements

The proposed MIMO antenna is practically implemented on Arlon AD270 ($\epsilon_r = 2.7$, $\tan\delta = 0.002$) copper-coated laminate and DR are made from ECCOSTOCK Hik dielectric slab and it is displayed in Fig. 7(a-b).

An Agilent N5230A vector network analyzer is used to perform S-parameters measurements and measured results are given in Fig. 7(c). Measured operating bandwidth is 0.45 GHz from 3.19 GHz to 3.64 GHz, where isolation between ports remains below 18 dB and it agrees well with simulation results. Simulated and measured gain vs frequency response of the MIMO antenna is plotted in Fig. 7(d). Mentioning the figure, frequency selective nature of the gain response with sharp roll-off in band-edge and four radiation dips outside passband assures the filtering performance of this MIMO configuration.

Flat in-band gain of 8.0 ± 0.25 dBi is obtained and suppression levels between in-band and out-of-band gain remain below -25 dB. Far-field radiation pattern of the filtering MIMO DRA array is plotted in Fig. 8 at 3.3 GHz and 3.4 GHz. Measurement is done by connecting one port with a power meter and terminating another port with a matched load. A good broadside directive pattern with a cross-polarization level below -25 dB is achieved both in E and H-plane. It is visible from Fig. 8 that the 3-dB beamwidth in the E-plane is approximately 105° . A more directive



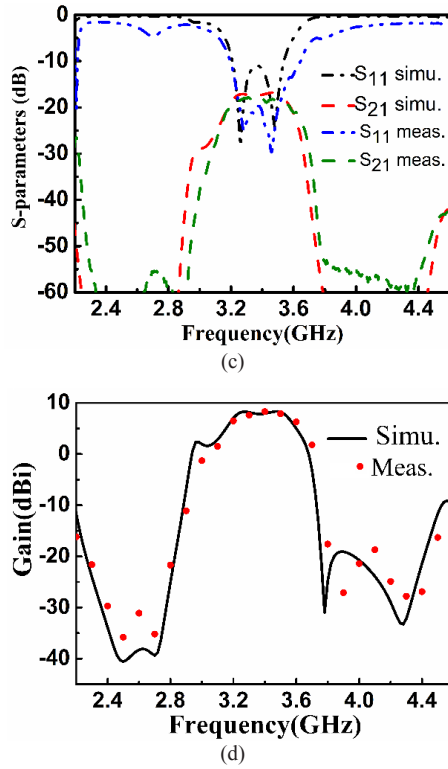


Fig. 7. Fabricated prototype for the proposed MIMO DRA array: (a) bottom view, (b) top view, (c) corresponding variation of simulated and measured S-parameters magnitude with frequency, (d) simulated and measured broadside gain with frequency.

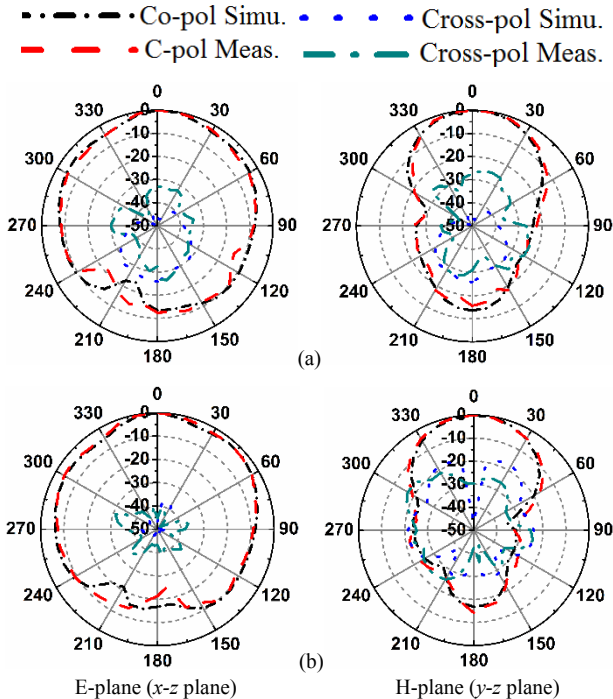


Fig. 8. Simulated and measured normalized radiation patterns for the proposed MIMO antenna along xz -plane and yz -plane at: (a) 3.3 GHz and (b) 3.4 GHz. (Port-1 is excited and Port-2 is terminated with matched load).

beam with beamwidth of 60° is obtained in H-plane as the proposed design behaves as 2-element H-plane linear array.

4. Diversity Performances

Diversity performance is needed to study along with the S-parameters and radiation patterns to understand the behavior of the antenna in MIMO application. Characterization of diversity performance is analyzed from envelope correlation coefficient (ECC), diversity gain (DG), channel capacity loss (CCL) and total reflection coefficient (TARC) values.

Information regarding correlation between the radiation patterns of two antenna elements is provided by ECC. Fundamental equation for calculation of ECC is based on radiation parameters. However, it is very complex process. Hence, broadband ECC calculation from the S-parameters is evaluated in [29]. Although, it is easy process, it can be applicable for well-matched and highly radiation efficient antennas. High radiation efficiency is the inherent characteristic of DRAs. As simulated efficiency of the proposed MIMO array is around 86% in the operating band, here ECC is computed from S-parameters based formula given in [30].

$$ECC = \rho_{e,ij} = \frac{|S_{ii}^* S_{ij} + S_{ji} S_{jj}^*|^2}{(1 - |S_{ii}|^2 - |S_{ij}|^2)(1 - |S_{jj}|^2 - |S_{ji}|^2)} \quad (3)$$

where S_{ii} is reflection coefficient and S_{ij} is mutual coupling between the MIMO ports. The simulated and measured ECC is shown in Fig. 9(a) and values are well below 0.01 throughout the operating range and hence satisfy the diversity criterion.

Diversity gain (DG) signifies the signal to noise improvement ratio with respect to the unit antenna element and it is computed using (4) given in [31]

$$DG = 10\sqrt{1 - ECC^2} \quad (4)$$

The DG values are depicted in Fig. 9(a) and it is > 9.99 dB in the operating band.

Channel capacity loss (CCL) is yet another noteworthy parameter for the characterization of MIMO system. CCL can be computed from S-parameter using (5–7) given in [31]

$$CCL = -\log_2(\Psi^R), \quad (5)$$

$$\Psi^R = [\rho_{ij}]; i, j = 1, 2 \quad (6)$$

where Ψ^R is receiving antenna correlation matrix and

$$\rho_{ii} = (1 - |S_{ii}|^2 - |S_{ij}|^2), \rho_{ij} = -(S_{ii}^* S_{ij} + S_{ji}^* S_{jj}); i, j = 1 \text{ or } 2. \quad (7)$$

The evaluated CCL values lie within the limit (i.e. < 0.5 bit/s/Hz) in the operating range as depicted in Fig. 9(b). As the value of this diversity parameter gives a satisfactory performance in the operating band and deteriorates sharply at band edges, it reflects excellent filtering MIMO characteristics.

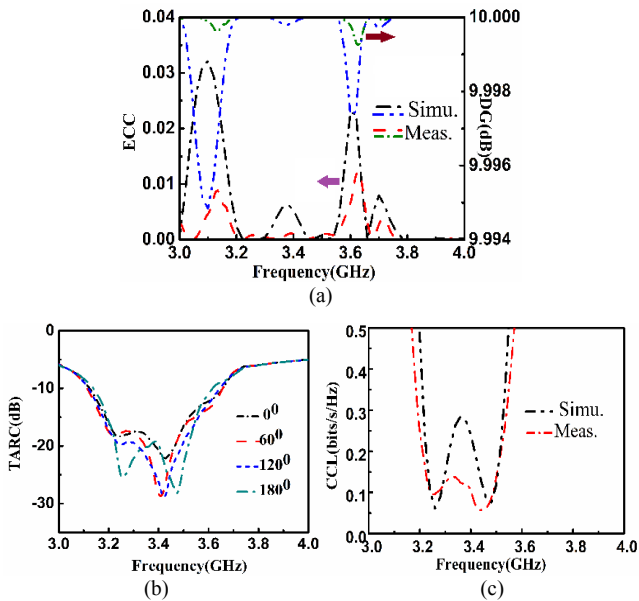


Fig. 9. Frequency variation of (a) Envelope Correlation Coefficient (ECC) & Diversity Gain (DG), (b) Channel Capacity Loss (CCL) and (c) measured Total Reflection Coefficient (TARC) for the proposed antenna.

Total active reflection coefficient (TARC) is the maximum attainable operating bandwidth when all the radiators in the MIMO system operate simultaneously. For an N -element MIMO system, TARC metrics can be constructed as per (8), (9), given in [31]

$$\Gamma_a^t = \frac{\sum_{i=1}^N |b_i|^2}{\sum_{i=1}^N |a_i|^2} \tag{8}$$

and $\mathbf{b} = \mathbf{S} \mathbf{a}$ (9)

where a_i and b_i denote the incident and reflected signal at the i^{th} port respectively, and \mathbf{S} represents the scattering matrix. As the resultant values are complex in nature, TARC values are evaluated for multiple relative phase angles (0° , 60° , 120° , 180°) and are depicted in Fig. 9(c). A stable response for all the phase angles with values below -10 dB is observed in the operating range. There is a little difference between experimental and simulated results in Fig. 9(a). The difference in measured and simulated results may arise due to the manual placement of the DR over the substrate and the use of adhesive material to append the dielectric resonator (DR) over the substrate. Though the measured results deviate a little from the simulation, the value of the diversity parameters remains in the threshold range and gives a satisfactory performance in the operating band.

Table 1 compares the proposed filtering MIMO DRA array with some recently reported MIMO DRA. It is apparent that the proposed design provides sound port isolation with excellent average broadside gain of 8 dBi. The proposed MIMO DRA array provides filtering gain characteristics hence it minimizes the out-of-band interference. It also offers exceptional ECC/CCL values within the operating band.

[Ref], Year	Array	Isolation (dB)	Avg. Gain (dBi)	ECC/CCL (bits/s/Hz)	Filtering
[34], 2015	N	18	N.A	<0.02/--	N
[35], 2019	N	18	4	<0.21/<0.3	N
[33], 2017	N	20	3	<0.16/<0.25	N
[27], 2019	N	25	6.2	<0.002/<0.2	N
[22], 2017	Y	>25	7	<0.002/--	N
This work	Y	20	8	<0.008/<0.3	Y

Tab.1. Performance comparison of MIMO DRA with the proposed work.

5. Conclusion

A high-gain MIMO DRA array with skirt filtering gain characteristics is studied in this paper. First, a two-element filtering DRA array is incorporated by amalgamating an input filtering stage (IFS) with a conventional T-junction power splitter. The array offers an average gain of 7.8 dBi in the operating band (3.2 GHz–3.54 GHz) with a sharp roll-off at band-edges. The presence of four-radiation dips outside the operating band enhances the frequency selectivity of the array with a noticeable amount of gain suppression (below -25 dB) outside the passband. This array is further utilized to configure a two-port MIMO DRA array. The proposed filtering MIMO DRA array is fabricated and tested to validate the simulation results. Measured results are in good agreement with the simulation results with an impedance bandwidth of 13% from 3.19 GHz to 3.64 GHz and port to port isolation of 20 dB. Its appropriateness as sub-6 GHz high gain frequency-selective MIMO array can be concluded from all the values of diversity parameters (ECC, DG, CCL), port isolation and gain response.

Acknowledgments

The authors thank senior colleagues for their valuable comments which have helped to improve the quality of paper.

Reference

[1] ZUO, J., CHEN, X., HAN, G., et al. An integrated approach to RF antenna-filter co-design. *IEEE Antennas and Wireless Propagation Letters*, 2009, vol. 8, p. 141–144. DOI: 10.1109/LAWP.2009.2012732

[2] LIM, ENG HOCK, LEUNG, KWOK WA. *Compact Multifunctional Antennas for Wireless Systems*. John Wiley & Sons, 2012. DOI: 10.1002/9781118243244

- [3] ALHEGAZI, A., ZAKARIA, Z., SHAIRI, N. A., et al. Compact UWB filtering-antenna with controllable WLAN band rejection using defected microstrip structure. *Radioengineering*, 2018, vol. 27, no. 1, p.110–117. DOI: 10.13164/re.2018.0110
- [4] WU, W.-J., YIN, Y.-Z., ZUO, S.-L., et al. A new compact filter-antenna for modern wireless communication systems. *IEEE Antennas and Wireless Propagation Letters*, 2011, vol. 10, p. 1131–1134. DOI: 10.1109/LAWP.2011.2171469
- [5] TANG, M.-C., SHI, T., ZIOLKOWSKI, R. W. Planar ultra-wideband antennas with improved realized gain performance. *IEEE Transactions on Antennas and Propagation*, 2015, vol. 64, no. 1, p. 61–69. DOI: 10.1109/TAP.2015.2503732
- [6] TANG, M.-C., CHEN, Y., ZIOLKOWSKI, R. W. Experimentally validated, planar, wideband, electrically small, monopole filtennas based on capacitively loaded loop resonators. *IEEE Transactions on Antennas and Propagation*, 2016, vol. 64, no. 8, p. 3353–3360. DOI: 10.1109/TAP.2016.2576499
- [7] LIN, C., CHUNG, S. A filtering microstrip antenna array. *IEEE Transactions on Microwave Theory and Techniques*, 2011, vol. 59, no. 11, p. 2856–2863. DOI: 10.1109/TMTT.2011.2160986
- [8] CHEN, F., HU, H., LI, R. et al. Design of filtering microstrip antenna array with reduced sidelobe level. *IEEE Transactions on Antennas and Propagation*, 2017, vol. 65, no. 2, p. 903–908. DOI: 10.1109/TAP.2016.2639469
- [9] MAO, C., GAO, S., WANG, Y., et al. An integrated filtering antenna array with high selectivity and harmonics suppression. *IEEE Transactions on Microwave Theory and Techniques*, 2016, vol. 64, no. 6, p. 1798–1805. DOI: 10.1109/TMTT.2016.2561925
- [10] PETOSA, A. *Dielectric Resonator Antenna Handbook*. Norwood (MA): Artech House, 2007. ISBN: 1596932066
- [11] BALLAV, S., PARUI, S. K. Aperture coupled dielectric resonator antenna embedded in a secondary substrate for mechanical firmness. *Radioengineering*, 2018, vol. 27, no. 3, p. 679–685. DOI: 10.13164/RE.2018.0679
- [12] HU, P. F., PAN, Y. M., ZHANG, X. Y., et al. A compact filtering dielectric resonator antenna with wide bandwidth and high gain. *IEEE Transactions on Antennas and Propagation*, 2016, vol. 64, no. 8, p. 3645–3651. DOI: 10.1109/TAP.2016.2565733
- [13] HU, P. F., PAN, Y. M., ZHANG, X. Y., et al. Broadband filtering dielectric resonator antenna with wide stopband. *IEEE Transactions on Antennas and Propagation*, 2017, vol. 65, no. 4, p. 2079–2084. DOI: 10.1109/TAP.2017.2670438
- [14] HU, P. F., PAN, Y. M., KWOK, WA LEUNG, et al. Wide-/dual-band omnidirectional filtering dielectric resonator antennas. *IEEE Transactions on Antennas and Propagation*, 2018, vol. 66, no. 5, p. 2622–2627. DOI: 10.1109/TAP.2018.2809706
- [15] PAN, Y. M., HU, P. F., KWOK, WA LEUNG, et al. Compact single-/dual-polarized filtering dielectric resonator antennas. *IEEE Transactions on Antennas and Propagation*, 2018, vol. 66, no. 9, p. 4474–4484. DOI: 10.1109/TAP.2018.2845457
- [16] LIU, Y.-T., KWOK WA LEUNG, REN, J., et al. Linearly and circularly polarized filtering dielectric resonator antennas. *IEEE Transactions on Antennas and Propagation*, 2019, vol. 67, no. 6, p. 3629–3640. DOI: 10.1109/TAP.2019.2902670
- [17] HU, P. F., PAN, Y. M., ZHANG, X. Y., et al. A compact quasi-isotropic dielectric resonator antenna with filtering response. *IEEE Transactions on Antennas and Propagation*, 2019, vol. 67, no. 2, p. 1294–1299. DOI: 10.1109/TAP.2018.2883611
- [18] SAHOO, A. K., GUPTA, R. D., PARIHAR, M. S. Circularly polarised filtering dielectric resonator antenna for X-band applications. *IET Microwaves, Antennas & Propagation*, 2018, vol. 12, no. 9, p. 1514–1518. DOI: 10.1049/iet-map.2017.1159
- [19] WANG, X.-Y., TANG, S.-C., SHI, X.-F., et al. A low-profile filtering antenna using slotted dense dielectric patch. *IEEE Antennas and Wireless Propagation Letters*, 2019, vol. 18, no. 3, p. 502–506. DOI: 10.1109/LAWP.2019.2895320
- [20] BALLAV, S., PARUI, S. K. Performance enhancement of dielectric resonator antenna by using cross-resonator based filtering feed-network. *AEU-International Journal of Electronics and Communications*, 2020, vol. 114, p. 1–8. DOI: 10.1016/j.aue.2019.152989
- [21] SAAD, A. A. R., MOHAMED, H. A. Printed millimeter-wave MIMO-based slot antenna arrays for 5G networks. *AEU-International Journal of Electronics and Communications*, 2019, vol. 99, p. 59–69. DOI:10.1016/j.aue.2018.11.029
- [22] SHARAWI, M. S., PODILCHAK, S. K., HUSSAIN, M. T., et al. Dielectric resonator based MIMO antenna system enabling millimetre-wave mobile devices. *IET Microwaves, Antennas & Propagation*, 2017, vol. 11, no. 2, p. 287–293. DOI: 10.1049/iet-map.2016.0457
- [23] SHARAWI, M. S., PODILCHAK, S. K., KHAN, M. U., et al. Dual-frequency DRA-based MIMO antenna system for wireless access points. *IET Microwaves, Antennas & Propagation*, 2017, vol. 11, no. 8, p. 1174–1182. DOI: 10.1049/iet-map.2016.0671
- [24] ZHANG, Y., DENG, J., LI, M., et al. A MIMO dielectric resonator antenna with improved isolation for 5G mm-wave applications. *IEEE Antennas and Wireless Propagation Letters*, 2019, vol. 18, no. 4, p. 747–751. DOI: 10.1109/LAWP.2019.2901961
- [25] BOUTEJDAR, A., IBRAHIM, A. A., ALI, W. A. E. Design of compact size and tunable band pass filter for WLAN applications. *Electronics Letters*, 2016, vol. 52, no. 24, p. 1996–1997. DOI: 10.1049/el.2016.3073
- [26] XUE, Q., JIN, J. Y. Bandpass filters designed by transmission zero resonator pairs with proximity coupling. *IEEE Transactions on Microwave Theory and Techniques*, 2017, vol. 65, no. 11, p. 4103–4110. DOI: 10.1109/TMTT.2017.2697878
- [27] SARKAR, G. A., BALLAV, S., CHATTERJEE, A., et al. Four-element MIMO DRA with high isolation for WLAN applications. *Progress in Electromagnetics Research Letters*, 2019, vol. 84, p. 99–106. DOI: 10.2528/PIERL19031304
- [28] FRITZ-ANDRADE, E., JARDON-AGUILAR, H., TIRADO-MENDEZ, J. A. Mutual coupling reduction of two 2x1 triangular-patch antenna array using a single neutralization line for MIMO applications. *Radioengineering*, 2018, vol. 27, no. 4, p. 976–982. DOI: 10.13164/re.2018.0976
- [29] SHARAWI, M. S., KHAN, M. U., NUMAN, A. B., et al. A CSRR loaded MIMO antenna system for ISM band operation. *IEEE Transactions on Antennas and Propagation*, 2013, vol. 61, no. 8, p. 4265–4274. DOI: 10.1109/TAP.2013.2263214
- [30] LI, J., CHU, Q., LI, Z., et al. Compact dual band-notched UWB MIMO antenna with high isolation. *IEEE Transactions on Antennas and Propagation*, 2013, vol. 61, no. 9, p. 4759–4766. DOI: 10.1109/TAP.2013.2267653
- [31] CHANDEL, R., GAUTAM, A. K., RAMBABU, K. Tapered fed compact UWB MIMO-diversity antenna with dual band-notched characteristics. *IEEE Transactions on Antennas and Propagation*, 2018, vol. 66, no. 4, p. 1677–1684. DOI: 10.1109/TAP.2018.2803134
- [32] CHOUKIKER, Y. K., SHARMA, S. K., BEHERA, S. K. Hybrid fractal shape planar monopole antenna covering multiband wireless communications with MIMO implementation for mobile handheld devices. *IEEE Transactions on Antennas and Propagation*, 2014, vol. 62, no. 3, p. 1483–1488. DOI: 10.1109/TAP.2013.2295213
- [33] DAS, G., SHARMA, A., GANGWAR, R. K. Dielectric resonator-based two-element MIMO antenna system with dual band

characteristics. *IET Microwaves, Antennas & Propagation*, 2017, vol. 12, no. 5, p. 734–741. DOI: 10.1049/iet-map.2017.0744

- [34] NASIR, J., JAMALUDDIN, M. H., KHALILY, M., et al. A reduced size dual port MIMO DRA with high isolation for 4G applications. *International Journal of RF and Microwave Computer-Aided Engineering*, 2015, vol. 25, no. 6, p. 495–501. DOI: 10.1002/mmce.20884
- [35] KUMARI, T., DAS, G., SHARMA, A., et al. Design approach for dual element hybrid MIMO antenna arrangement for wideband applications. *International Journal of RF and Microwave Computer-Aided Engineering*, 2019, vol. 29, no. 1, p. 1–10. DOI: 10.1002/mmce.21486

About the Authors ...

Suparna BALLAV received the B.Sc. (Physics Hons) degree in 2011 and the B.Tech. and M.Tech in Radio Physics and Electronics from University of Calcutta, India in the year 2014 and 2016, respectively. She is pursuing Ph.D. degree in Microwave Engineering at the Department Electronics and Tele-communication Engineering, Indian Institute of Engineering Science and Technology (IEST), Shibpur, West Bengal, India since August 2016. Her research interests include dielectric resonators for microwave circuits and antenna application.

Goffar Ali SARKAR was born in 1994. He received B.Tech. degree in Electronics and Communication Engi-

neering from Aliah University in 2015 and M.Tech. degree in Electronics and Telecommunication Engineering with specialization on Microwave Communication from IEST, Shibpur in 2017. He is currently working as a Ph.D. Scholar at IEST, Shibpur. His research interest includes analysis and design of microstrip antennas and arrays, dielectric resonator antennas and arrays, MIMO antennas, SIW antennas, etc.

Susanta Kumar PARUI received the B.Sc. degree in Physics and B.Tech. degree in Radio Physics and Electronics from University of Calcutta, India in the year 1987 and 1990 respectively and the Ph.D. degree in Microwave Engineering from the Bengal Engineering and Science University (presently known as the Indian Institute of Engineering Science and Technology), Shibpur, India. From 1993 to 2000, he was an Instrument Engineer in process control industries. Since 2000, he has been associated with the Department of Electronics and Tele-Communication Engineering, Indian Institute of Engineering Science & Technology, Shibpur and presently holds the post of Professor. He is the author of more than 60 papers in referred journals and conference proceedings. His research interests include planar circuits, antennas, SIW, DGS, EBG, FSS and metamaterials. Dr. Parui was awarded post doctoral fellowship from the Royal Academy of Engineering, U.K in the year 2009.